1521-0111/97/3/212–225$35.00
MOLECULAR PHARMACOLOGY

https://doi.org/10.1124/mol.119.117887
Mol Pharmacol 97:212–225, March 2020

The Peroxisome Proliferator–Activated Receptor (PPAR)-γ Antagonist 2-Chloro-5-Nitro-N-Phenylbenzamide (GW9662) Triggers Perilipin 2 Expression via PPARδ and Induces Lipogenesis and Triglyceride Accumulation in Human THP-1 Macrophages[S]

Martin Schubert,[1] Stefanie Becher,[1] Maria Wallert, Marten B. Maeß, Masoumeh Abhari, Knut Rennert, Alexander S. Mosig, Silke Große, Regine Heller, Michael Grün,[2] and Stefan Lorkowski

Institute of Nutrition, Friedrich Schiller University Jena, Jena, Germany (M.S., S.B., M.W., M.B.M., M.A., M.G., S.L.); Competence Cluster for Nutrition and Cardiovascular Health (nutriCARD), Halle-Jena-Leipzig, Germany (M.S., M.W., M.G., S.L.); Institute of Biochemistry II, Jena University Hospital, Jena, Germany (K.R., A.S.M.); and Institute of Molecular Cell Biology, Center for Molecular Biomedicine (CMB), Jena University Hospital and Friedrich Schiller University Jena, Jena, Germany (S.G., R.H.)

Received July 29, 2019; accepted December 6, 2019

ABSTRACT

Peroxisome proliferator-activated receptors (PPARs) are members of the nuclear hormone receptor family, playing pivotal roles in regulating glucose and lipid metabolism as well as inflammation. While characterizing potential PPARγ ligand activity of natural compounds in macrophages, we investigated their influence on the expression of adipophilin [perilipin 2 (PLIN2)], a well-known PPARγ target. To confirm that a compound regulates PLIN2 expression via PPARγ, we performed experiments using the widely used PPARγ antagonist 2-chloro-5-nitro-N-phenylbenzamide (GW9662). Surprisingly, instead of blocking upregulation of PLIN2 expression in THP-1 macrophages, expression was concentration-dependently induced by GW9662 at concentrations and under conditions commonly used. We found that this unexpected upregulation occurs in many human and murine macrophage cell models and also primary cells. Profiling expression of PPAR target genes showed upregulation of several genes involved in lipid uptake, transport, and storage as well as fatty acid synthesis by GW9662. In line with this and with upregulation of PLIN2 protein, GW9662 elevated lipogenesis and increased triglyceride levels. Finally, we identified PPARδ as a mediator of the substantial unexpected effects of GW9662. Our findings show that: 1) the PPARγ antagonist GW9662 unexpectedly activates PPARδ-mediated signaling in macrophages, 2) GW9662 significantly affects lipid metabolism in macrophages, 3) careful validation of experimental conditions and results is required for experiments involving GW9662, and 4) published studies in a context comparable to this work may have reported erroneous results if PPARγ independence was demonstrated using GW9662 only. In light of our findings, certain existing studies might require reinterpretation regarding the role of PPARγ.

SIGNIFICANCE STATEMENT

Peroxisome proliferator–activated receptors (PPARs) are targets for the treatment of various diseases, as they are key regulators of inflammation as well as lipid and glucose metabolism. Hence, reliable tools to characterize the molecular effects of PPARs are indispensable. We describe profound and unexpected off-target effects of the PPARγ antagonist 2-chloro-5-nitro-N-phenylbenzamide (GW9662) involving PPARδ and in turn affecting macrophage lipid metabolism. Our results question certain existing studies using GW9662 and make better experimental design of future studies necessary.

Introduction

A common strategy for the elucidation of signaling pathways mediating the effects of a compound of interest is the use of specific chemical agonists or antagonists for signaling proteins. GW9662, known as a selective peroxisome proliferator (PPAR)γ antagonist, is widely accepted to demonstrate participation of PPARγ in signaling cascades (Leesnitzer et al., 2002; Lea et al., 2004; Nielsen et al., 2006).

PPARγ, together with PPARα and PPARδ (also termed PPARβ), constitute the PPAR subfamily of nuclear receptors. PPARs are activated by a variety of molecules and act mainly as sensors for fatty acids and fatty acid–derived metabolites (Lefebvre et al., 2006; Tontonoz and Spiegelman, 2008; Neels and Grimaldi, 2014). As transcription factors, PPARs regulate various genes implicated in lipid and glucose metabolism, inflammation, proliferation, and differentiation (Varga et al., 2011; Vrablík and Češka, 2015).

[1]M.S. and S.B. contributed equally to this work.
[2]Current affiliation: QMP, Jena, Germany.
https://doi.org/10.1124/mol.119.117887.
[S] This article has supplemental material available at molpharm.aspetjournals.org.

The PPAR subtypes differ in their expression levels in tissues, their affinity for their respective ligands, and their biologic functions. PPARα and PPARδ are related to lipid metabolism because of their key role in the regulation of fatty acid oxidation and lipoprotein metabolism (Luquet et al., 2005; Lefebvre et al., 2006). Furthermore, anti-inflammatory effects and regulatory roles in glucose metabolism have been reported for both isoforms (Lefebvre et al., 2006; Neels and Grimaldi, 2014; Magadum and Engel, 2018). While PPARδ is ubiquitously expressed (most abundantly in tissues with high fatty acid metabolism) (Neels and Grimaldi, 2014), PPARα is mainly found in liver and muscles (Lefebvre et al., 2006). PPARγ is predominantly expressed in adipose tissue and plays a central role in adipogenesis (Wang, 2010). In addition, PPARγ exerts considerable effects on lipid and glucose metabolism and insulin sensitivity (Tontonoz and Spiegelman, 2008). Based on the knowledge of their physiologic roles, PPARs represent interesting targets for the treatment of various diseases. In brief, fibrates, agonists of PPARα, have been used as hypolipidemic drugs to treat hypertriglyceridemia (Vrablík and Češka, 2015); PPARδ is regarded as a promising target for the treatment of metabolic syndrome because of its positive effects on serum cholesterol and lipid profiles (Neels and Grimaldi, 2014); and the insulin-sensitizing effects of thiazolidinediones, a class of PPARγ ligands, are used for the treatment of type 2 diabetes mellitus (Tontonoz and Spiegelman, 2008; Hong et al., 2018).

Crucial for the use of PPARs as pharmacological targets is the understanding of their modes of action. Thus, several models have been described for PPAR-dependent gene regulation (Varga et al., 2011) as well as the functional regulation of PPARs (Brunmeir and Xu, 2018). The most common model for PPAR-dependent gene regulation is the direct transcriptional regulation by heterodimerization of a PPAR isoform with retinoid X receptors. In the absence of ligands, the heterodimer is bound to the so-called PPAR response element in the promoter of target genes. In this state, the heterodimer binds a corepressor complex and represses the transcription of target genes. Upon ligand binding, the corepressor complex is replaced by coactivators, resulting in the transcription of PPAR target genes. Chemical antagonists bind to the respective PPAR isoform, leading to the maintenance of the corepressor complex and to the prevention of agonist binding (Harmon et al., 2011). Thus, chemical antagonists are considered as useful tools in PPAR research, especially for the verification of possible PPAR ligands.

A commonly used chemical antagonist in PPAR research is GW9662. GW9662 has been shown to covalently and irreversibly bind to the PPARγ ligand binding pocket (Leesnitzer et al., 2002; Brust et al., 2018). The binding of activating ligands is thereby prevented, and the signal transduction via PPARγ is interrupted. Surprisingly, GW9662 did not act as expected in our hands when used in commonly reported concentrations and incubation periods in the THP-1 macrophage model system. Here, GW9662 did not diminish the expression of the PPARγ target genes perilipin 2 (PLIN2) and cluster of differentiation 36 (CD36) induced by established PPARγ agonists, such as rosiglitazone or 15-deoxy-$\Delta^{12,14}$-prostaglandin J_2 (15dPGJ2). Unexpectedly, these target genes were upregulated in THP-1 macrophages by GW9662 itself. This effect was not restricted to THP-1 cells but was also observed in several other human and murine macrophage cell lines. Our study clearly shows that the suitability of GW9662 as a tool for the investigation of PPARγ-dependent signaling pathways is questionable. This work aims, therefore, to characterize: 1) the effect of GW9662 on gene and protein expression as well as overall cellular function of macrophages and 2) the underlying mechanism of the unexpected effects of GW9662 in macrophages.

The importance of PPARs as therapeutic targets in several diseases requires scrupulous investigation of PPAR signaling using reliable experimental tools. Our study is exploratory research that will therefore help to correctly interpret the variety of results obtained by the use of GW9662 in the future, especially in macrophage model systems.

Materials and Methods

Ethics Statement. Mononuclear cells were isolated from buffy coats obtained from peripheral blood of anonymized healthy male and/or female volunteers. Blood donors were informed about the aim of the study and gave written informed consent. The procedure was approved by the ethics committee of the University Hospital Jena (2446-12/08) and conducted according to the ethical principles defined by the declaration of Helsinki. Animal procedures, including isolation of peritoneal macrophages, were approved by the Animal Care and Use Committee of Thuringia (permit number 02-003/09) and were in line with the National Institutes of Health guidelines for the care and use of laboratory animals.

Reagents. Chemicals were from Roth (Karlsruhe, Germany), Sigma-Aldrich (Seelze, Germany), and Merck Chemicals (Darmstadt, Germany) if not otherwise indicated. Rosiglitazone, 15dPGJ2, 4-chloro-*N*-[2-[[5-(trifluoromethyl)-2-pyridinyl]sulfonyl]ethyl]benzamide (GSK3787), and 2-chloro-5-nitro-N-4-pyridinyl-benzamide (T0070907) were purchased from Cayman Chemical Company (Biomol, Hamburg, Germany). GW9662 was purchased either from Sigma-Aldrich or Enzo Life Sciences (Lörrach, Germany). Key findings were confirmed using different lots of GW9662 obtained either from Sigma-Aldrich or Enzo Life Sciences.

Cell Culture. Murine RAW264.7 and J774A.1 cells as well as human THP-1 and U937 cells were obtained from American Type Culture Collection (Manassas, VA). Cells were maintained as recommended by the supplier and cultured at 37°C in a humidified 5% CO_2 air atmosphere. THP-1 and U937 monocytes were differentiated into macrophages using 100 ng/ml phorbol-12-myristate-13-acetate (PMA; Sigma-Aldrich) in the presence of 50 μM β-mercaptoethanol (Sigma-Aldrich) in RPMI 1640 medium (PAA, Cölbe, Germany) supplemented with 10% FBS Gold (PAA) and antibiotics (PAA) for 96 hours as previously described (Robenek et al., 2005). Murine cells were

ABBREVIATIONS: 15dPGJ2, 15-deoxy-$\Delta^{12,14}$-prostaglandin J_2; CD36, cluster of differentiation 36; COX, cyclooxygenase; FABP, fatty acid–binding protein; GPR, Global Pattern Recognition; GSK3787, 4-chloro-*N*-[2-[[5-(trifluoromethyl)-2-pyridinyl]sulfonyl]ethyl] benzamide; GW9662, 2-chloro-5-nitro-N-phenylbenzamide; J774, murine macrophages cell line from BALB/C mice; PBMC, peripheral blood mononuclear cells; PCR, polymerase chain reaction; PLIN2, perilipin 2; PMA, phorbol-12-myristate-13-acetate; PPAR, peroxisome proliferator–activated receptor; Ppib, peptidyl-prolyl cis-trans isomerase B; RAW264.7, murine leukemic monocyte macrophage cell line; RPL37A, ribosomal protein L37a; RT-qPCR, quantitative real-time reverse-transcription PCR; siRNA, small interfering ribonucleic acid; T0070907, 2-chloro-5-nitro-N-4-pyridinyl-benzamide; THP-1, human monocytic cell line; U937, human monocytic cells from histiocytic lymphoma; VLDL, very low-density lipoprotein.

cultivated in Dulbecco's modified Eagle's medium high-glucose medium (PAA) supplemented with 10% FBS and antibiotics according to the supplier's instructions. All cell lines were routinely tested for mycoplasma contamination using the mycoplasma detection kit PP-401 (Jena Bioscience, Jena, Germany) based on a PCR reaction. Cells were incubated with various compounds in serum-free medium with concentrations and for times as indicated in the figures.

Isolation of Mouse Peritoneal Macrophages. Male C57BL/6J mice at the age of 27–34 weeks were purchased from Jackson Laboratories (Bar Harbor, ME). All animal procedures were approved by the Animal Care Committee of the federal state Thuringia (Germany). Mouse peritoneal macrophages were isolated as previously described (Zhang et al., 2008). Peritoneal macrophages were obtained by peritoneal lavage. For this, mice were anesthetized with isoflurane (DeltaSelect, Dreireich, Germany) and sacrificed with CO_2. The abdomen was soaked with 70% ethanol and opened, and the peritoneal cavity was washed twice with 5 ml Hank's balanced salt solution containing 500 μM EDTA. The liquid that includes peritoneal macrophages was extracted with a syringe and collected in an ice-cold tube. The suspension was centrifuged at 300*g* for 10 minutes at 4°C; the pellet was resuspended in 2 ml RPMI 1640 medium supplemented with antibiotics and 10% FBS, and cells were plated in 24-well plates. Cells were incubated for 2 hours at 37°C in a humidified air atmosphere with 5% CO_2 and were then washed five times with medium to remove nonadherent cells (Kim et al., 2005). After resting the cells for another 24 hours in serum containing RPMI 1640 at 37°C, the medium was replaced by serum-free RPMI 1640, and macrophages were cultured in the presence or absence of compounds for the times and concentrations indicated.

Isolation and Maturation of Peripheral Blood Mononuclear Cells. Mononuclear cells were isolated from buffy coats obtained from peripheral blood of anonymized healthy male and/or female volunteers. Buffy coat blood was diluted 1:1 with PBS (PAA), layered onto Lymphocyte Separation Medium (LSM) 1077 (1.077 g/ml; ratio 1:1; PAA), and centrifuged at 1200*g* for 20 minutes at 20°C (Gruen et al., 2004). The peripheral blood mononuclear cell (PBMC)-containing interphase was collected, washed three times with PBS, and resuspended in RPMI 1640 containing 10% FBS. Cells were plated in 25-cm^2 flasks in RPMI 1640 medium including supplementations. After 2 hours at 37°C in an air atmosphere containing 5% CO_2, adherent cells were washed twice with serum-free medium and were differentiated into macrophages for 8 days in RPMI 1640 supplemented with antibiotics and 20% human serum. PBMC-derived macrophages were then stimulated as indicated in the figures.

RNA Isolation and cDNA Synthesis. Preparation of samples was conducted according to established protocols (Schnoor et al., 2009). Total RNA was prepared from cell lysates using RNeasy Mini Kit (Qiagen, Hilden, Germany) according to manufacturer's instructions, including an on-column DNAse I digestion (Qiagen) as previously reported (Stolle et al., 2007). Adequate RNA quality was assessed by agarose gel electrophoresis, and RNA was quantified photometrically. RevertAid First Strand cDNA Synthesis Kit (Fermentas, St. Leon-Rot, Germany) was used for reverse transcription of mRNA into cDNA as previously described (Stolle et al., 2005; Maeß et al., 2014). For each cDNA synthesis, 5 μg total RNA and 0.5 μg oligo (dT) primers were used. Finally, cDNA samples were diluted 10-fold and stored at −30°C prior to PCR analyses.

Quantitative Real-Time Reverse-Transcription PCR. Primer pairs (Supplemental Tables 1 and 2) for quantitative real-time reverse-transcription PCR (RT-qPCR) were designed using PrimerExpress software version 2.0.0 (Applied Biosystems, Weiterstadt, Germany) and were purchased from Invitrogen (Karlsruhe, Germany). Expression analyses by means of RT-qPCR were performed with QuantiTect SYBR Green PCR Kit (Qiagen) on a LightCycler 480 II instrument (Roche Diagnostics, Mannheim, Germany) as previously reported (Maess et al., 2010; Maeß et al., 2014). PCR runs consisted of a preincubation at 95°C for 15 minutes and 40 cycles of a two-step PCR, comprising a denaturing phase at 94°C for 15 seconds and a combined annealing and extension phase at 60°C for 30 seconds. Following PCR, a melting curve was recorded to estimate purity of the PCR product. PCR results were analyzed using the LightCycler software release version 1.5.0.39 (Roche Diagnostics). The fit point algorithm of the LightCycler software was used to calculate C_t values. Fold changes were calculated using Microsoft Excel 2007. RPL37A and Ppib were used as reference genes for human and murine cell lines, respectively (Maess et al., 2010, 2011). Samples were prepared in biologic replicates, and analyses were performed as technical duplicates as indicated.

Human PPAR Signaling 384 StellARray qPCR Arrays. For profiling the regulation of gene expression by GW9662, the Human PPAR Signaling 384 StellARray qPCR Arrays (Lonza, Basel, Switzerland) were used. Samples obtained from five independent experiments were pooled in equal proportions, and RT-qPCR analyses were performed with QuantiTect SYBR Green PCR Kit (Qiagen) on a Roche LightCycler 480 II instrument as previously outlined (Maess et al., 2010), with slight modifications according to Lonza's 384 StellARray qPCR Arrays manual. PCR runs consisted of a step for dissolving primers at 50°C for 2 minutes, a preincubation step at 95°C for 15 minutes, and 40 cycles of a two-step PCR composed of a denaturing phase at 94°C for 15 seconds and a combined annealing and extension phase at 60°C for 30 seconds. Following PCR cycles, melting curves were recorded to validate specificity of the PCR. PCR results were analyzed using the LightCycler software release version 1.5.0.39, and obtained raw data were imported to Lonza Global Pattern Recognition (GPR) Data Analysis Tool for calculation of fold changes. HSP90AA1 (cytosolic heat shock protein 90 kDa α, class A, member 1), HMOX1 (heme oxygenase 1), SLC22A5 (solute carrier family 22 (organic cation/carnitine transporter) member 5), HRAS (Harvey rat sarcoma viral oncogene homolog), NR2C1 (nuclear receptor subfamily 2, group C, member 1), MECR (mitochondrial *trans*-2-enoyl-CoA reductase), MED14 (mediator complex subunit 14), ELOVL3 (elongation of very long chain fatty acids (FEN1/Elo2, SUR4/Elo3, yeast)-like 3), and UBC (ubiquitin C) were identified as stably expressed by GPR Data Analysis Tool, and the geometric mean of these reference genes was used for normalization as recommended by the GPR Data Analysis Tool and following the instructions of the manufacturer.

Data Retrieval. Regulatory signaling pathways and biologic functions were assigned to genes whose expression was measured using Human PPAR Signaling 384 StellARray qPCR arrays as illustrated in Supplemental Table 3. For this assignment, National Center for Biotechnology Information, Kyoto Encyclopedia of Genes and Genomes, Reactome, and ARIADNE Genomic databases were systematically searched; information for assignment was collected and filtered manually. Gene names and their synonyms were retrieved from these databases. Genes were finally categorized manually according to their regulation of expression using a cutoff of 1.5 into "upregulated", "downregulated", "unchanged", and "not expressed/detected" and their role in metabolic and regulatory pathways.

Western Blot Analysis. Preparation of samples and Western blotting were conducted as previously reported (Wallert et al., 2015), but the transfer buffer contained 0.25 M Tris, 1.92 M glycine, 1% SDS, and 20% methanol (pH 8.3). Cells were harvested using a nondenaturing buffer (50 mM Tris-HCl, 0.5% Nonidet P40, 250 mM NaCl, 5 mM EDTA, 50 mM NaF, 0.5 mM Na_3VO_4) containing 1% protease inhibitor (Abcam, Cambridge, UK) and were processed for Western blotting. The antibody against PLIN2 (mouse anti-adipophilin clone AP125) was purchased from Progen (Heidelberg, Germany) and against α-tubulin (mouse anti-α-tubulin clone B-5-1-2) from Sigma-Aldrich. Secondary antibody (rabbit anti-mouse labeled with horseradish peroxidase) was from DAKO (Hamburg, Germany). For enhancing chemoluminescence signals for PLIN2, SignalBoost Immunreaction Enhancer Kit (Calbiochem, Darmstadt, Germany) was used. For detection, Pierce ECL Western Blotting Substrate and CL-XPosure Films (Thermo Fisher Scientific, Rockford, IL) were applied. Blots were analyzed densitometrically using ImageJ software version 1.4.3.67 (National Institutes of Health, Bethesda, MD).

Fluorescence Microscopy. Cells were cultured on coverslips as described above and incubated with compounds as indicated in the figures. After washing with PBS, cells were fixed with 4% paraformaldehyde in PBS and processed according to established protocols (Buers et al., 2009). The primary antibody against PLIN2 (Progen mouse anti-adipophilin clone AP125) was diluted 1:500, and the secondary antibody (Alexa Fluor 555 goat anti-mouse; Invitrogen) was used in a dilution of 1:200. Nuclei were stained using Hoechst Dye 33258 (Invitrogen) in a 1:10 dilution. Confocal images were acquired with a Zeiss LSM 510 confocal laser-scanning microscope; files were processed using Zeiss LSM Image Browser software version 3.1 (Carl Zeiss AG, Oberkochen, Germany), and fluorescence intensity was quantified using ImageJ software version 1.4.3.67.

Measurement of Cellular Triglyceride and Cholesterol Content. Mature THP-1 macrophages were incubated in the absence or presence of 10 μM GW9662 for 24 and 48 hours. Cells were harvested with 5% Triton X-100 (Sigma-Aldrich) in H_2O and prepared for enzymatic triglyceride and cholesterol analysis as follows. The cell suspension was sonicated three times on ice (electronic Sonopuls GM70; Bandelin, Berlin, Germany). An aliquot was taken for protein quantification using BCA Protein Assay (Thermo Scientific). Remaining samples were heated to 80°C for 10 minutes, incubated under slight shaking at that temperature for another 5 minutes, and rested at room temperature for cooling down. This process was repeated twice before samples were centrifuged. For analyzing triglyceride and cholesterol content, CHOD-PAP Kit from Roche Diagnostics and Triglyceride Assay Kit (Cayman Chemical Company) were applied according to manufacturer's instructions. Absorption was measured at 544 nm on a FLUOstar OPTIMA instrument (software version 2.10 R2; BMG Labtech, Ortenberg, Germany). Total cholesterol and triglyceride levels were normalized to intracellular protein amount.

Measurement of Lipogenesis by ^{14}C-Acetate Incorporation in Macrophages. For investigating the influence of GW9662 on lipid synthesis, mature THP-1 macrophages seeded into a 12-well-plate were incubated with 10 μM GW9662 or solvent for 20 hours and with 0.5 μCi/ml ^{14}C-labeled sodium acetate (Hartmann Analytic, Braunschweig, Germany) (specific activity of 57 mCi/mmol) for another 4 hours in serum-free RPMI 1640 medium containing 50 μM β-mercaptoethanol, 100 ng/ml PMA, 0.25% free fatty acid-free bovine serum albumin (Sigma-Aldrich), 500 pM biotin (Sigma-Aldrich), and 50 μM L-carnitin (Sigma-Aldrich). As negative control, cells were stimulated with 50–100 μM C75 (Sigma-Aldrich) for 6 hours to inhibit fatty acid synthesis. All samples were performed and analyzed in duplicates. After incubation, cells were washed three times with ice-cold HEPES/Ca^{2+} buffer (pH 7.4) and harvested using 0.2 ml 50 mM Tris buffer (pH 7.5) (AppliChem, Darmstadt, Germany). After adding 0.5 ml methanol (AppliChem) and 0.25 ml chloroform (Sigma-Aldrich) for lipid extraction, samples were thoroughly mixed and incubated for 15 minutes at room temperature. Then, 0.25 ml chloroform and 0.25 ml 0.1 M potassium chloride (Sigma-Aldrich) were added. To enhance extraction of free fatty acids, the pH of samples was lowered by adding 2 μl 1 M citric acid (Sigma-Aldrich). Samples were incubated for 5 minutes at room temperature and centrifuged for 5 minutes at 400*g* for phase separation. After transferring the lower phase, chloroform was vaporized, and lipids were solubilized with 0.5 ml 1% Triton X-100. After adding scintillation cocktail (Carl Roth), radioactivity was measured using a Liquid Scintillation Counter LSC Wallac 1410 (Pharmacia-Wallac, Turku, Finland), and the amount of incorporated ^{14}C-acetate was determined. Protein content of cell lysates was analyzed using the Lowry method, and ^{14}C-acetate incorporation was normalized to protein content.

Flow Cytometric Analysis of Apoptosis and Necrosis. To investigate whether THP-1 macrophages were undergoing apoptosis and necrosis in response to GW9662, cells were incubated with increasing doses of GW9662 as indicated in Supplemental Fig. 1 and stained with annexin V and 7-aminoactinomycin D (BD Biosciences, Heidelberg, Germany). In brief, after detaching cells with Accutase I (PAA), cells were washed twice with ice-cold PBS and incubated in binding-buffer containing annexin V and 7-aminoactinomycin D for 15 minutes in the dark. Samples were then diluted with binding buffer. Positive cells were analyzed flow cytometrically using a Beckman Coulter EPICS XL-MCL (Krefeld, Germany) and quantified using WinMDI software version 2.8 (Scripps Research Institute, La Jolla, CA).

Transfection. THP-1 monocytes were differentiated for 24 hours using 100 ng/ml PMA in the presence of 50 μM β-mercaptoethanol in RPMI 1640 medium supplemented with 10% FBS and antibiotics. Premature THP-1 cells were detached using Accutase I. Transfection was performed using Lonza's Human Monocyte Nucleofector Kit. Here, cells were resuspended in Nucleofector solution and transferred to a Nucleofector cuvette together with 0.25 μg silencer select siRNA (either s10880 PPARA, s10883 PPARD, s10888 PPARG, or Silencer Select Negative Control No. 2 siRNA; Life Technologies, Darmstadt, Germany). Nucleofection was carried out using program Y-001 in a Nucleofector 2b device. Next, cells were transferred to Lymphocyte Growth Medium-3 (Lonza) supplemented with 1% (v/v) nonessential amino acids (Lonza), 1% (v/v) sodium pyruvate (Sigma-Aldrich), and 1% human serum (Sigma-Aldrich) for 6 hours allowing reattachment. Subsequently, medium was replaced by Lymphocyte Growth Medium-3 supplemented with 1% (v/v) nonessential amino acids, 1% (v/v) sodium pyruvate, and 0.1% human serum. Cells were incubated 72 hours after transfection with GW9662 or vehicle for an additional 24 hours and subsequently harvested for RT-qPCR analysis as described. Transfection efficiency was determined after the 24-hour incubation period by RT-qPCR (Supplemental Fig. 14).

Data Presentation and Statistical Analyses. Data are presented as means ± S.E.M. by circles. Data of the respective individual independent experiments are represented by squares to provide information on variability of the data. Experiments were performed at least three times. In the case of high variability in the results, additional biologic replicates were performed to generate a meaningful result. Information on the times an experiment was performed are given in the respective figure legends, and the group sizes are always equal within the experiment and resemble the times the experiment was performed.

RT-qPCR data were analyzed based on the $2^{-\Delta\Delta ct}$ method, with controls set to one in each independent experiment. Presentation of individual data points (squares) was thus omitted for controls in RT-qPCR experiments.

Statistical analyses aim at the description of differences in the mean effect of treatments in individual experiments and were performed using OriginLab's OriginPro 9.1G. Appropriate statistical tests were chosen based on the experimental design and are indicated in the respective figure legends. $P < 0.05$ was considered statistically significant.

Results

While screening for potential PPARγ agonist activity of selected natural compounds, we intended to use PLIN2, a known PPARγ target gene (Gupta et al., 2001; Hodgkinson and Ye, 2003), as a readout. Blocking experiments using the widely used selective PPARγ antagonist GW9662 would confirm that regulation of PLIN2 mRNA expression by a compound of interest is mediated via PPARγ. Surprisingly, GW9662 exhibited unexpected effects on the expression of PLIN2 and other PPARγ target genes. Instead of blocking the expression of PLIN2 in THP-1 macrophages, the expression was induced by GW9662 at concentrations and under conditions widely used in studies published so far (Lea et al., 2004; Kourtidis et al., 2009). Therefore, we decided to investigate this phenomenon more systematically.

GW9662 Does Not Block Upregulation of PLIN2 Expression by Rosiglitazone and 15dPGJ2. Before starting to investigate the PPARγ participation in the signaling of the natural compounds of our interest, we conducted

a proof-of-concept, i.e., the combination of well-known PPARγ agonists with GW9662 and the use of known PPARγ target genes as readout. PLIN2 is a member of the family of perilipin, adipophilin, and TIP47 proteins and is one of the best investigated proteins involved in lipid storage in macrophages (Bickel et al., 2009). It has been shown to be regulated by PPARγ in macrophages (Hodgkinson and Ye, 2003). The scavenger receptor CD36 is pivotal in promoting macrophage foam cell formation (Nicholson and Hajjar, 2004) and is also a well-known PPARγ target gene (Chawla et al., 2001; Moore et al., 2001). Consequently, expression of PLIN2 and CD36 is induced by PPARγ ligands, such as rosiglitazone and 15dPGJ2 (Chawla et al., 2001; Hodgkinson and Ye, 2003). The confirmed PPARγ antagonist GW9662 (Leesnitzer et al., 2002; Seimandi et al., 2005) should block this induction. We therefore investigated the effect of GW9662 on rosiglitazone- and 15dPGJ2-induced expression of PLIN2 and CD36.

THP-1 macrophages were pretreated with 10 μM GW9662 in serum-free medium for 1 hour before incubating the cells with synthetic or natural PPARγ agonists rosiglitazone and 15dPGJ2 for another 24 hours. After harvesting the cells, total RNA was isolated and transcribed into cDNA for measuring relative mRNA expression levels of PLIN2 and CD36 using RT-qPCR. As expected, both 5 μM rosiglitazone and 5 μM 15dPGJ2 significantly induced the expression of PLIN2 mRNA to the 2.0-fold ($P < 0.05$) and to the 7.7-fold ($P < 0.001$), respectively (Fig. 1, top). Similarly, as shown in Fig. 1 (middle), expression of CD36 was significantly increased to the 3.5-fold ($P < 0.01$) and to the 7.8-fold ($P < 0.001$), respectively. Expression of the reference gene RPL37A was not affected and was used for normalization (Fig. 1, bottom). Surprisingly, treatment of THP-1 macrophages with 10 μM GW9662 significantly increased expression of PLIN2 and CD36 by more than the 2.1-fold ($P < 0.05$ and $P < 0.01$, respectively; Fig. 1, top and middle). Further data shown in Fig. 1 (top and middle) illustrate that pretreatment with 10 μM GW9662 abolished neither the effect of rosiglitazone nor of 15dPGJ2. Instead of repressing PPARγ ligand-induced expression of PLIN2 and CD36, GW9662 pretreatment significantly enhanced the effect of rosiglitazone (Fig. 1A) but did not alter induction by 15dPGJ2 (Fig. 1B). Interestingly, the synergistic effects were not limited to rosiglitazone but also observable for troglitazone. Troglitazone increased PLIN2 and CD36 gene expression like rosiglitazone and 15dPGJ2, and GW9662 did not block the effect (Supplemental Fig. 2). Pretreatment of THP-1 macrophages with GW9662 as well as incubating the cells in combination with agonist and antagonist at the same time for 24 hours also led to augmented

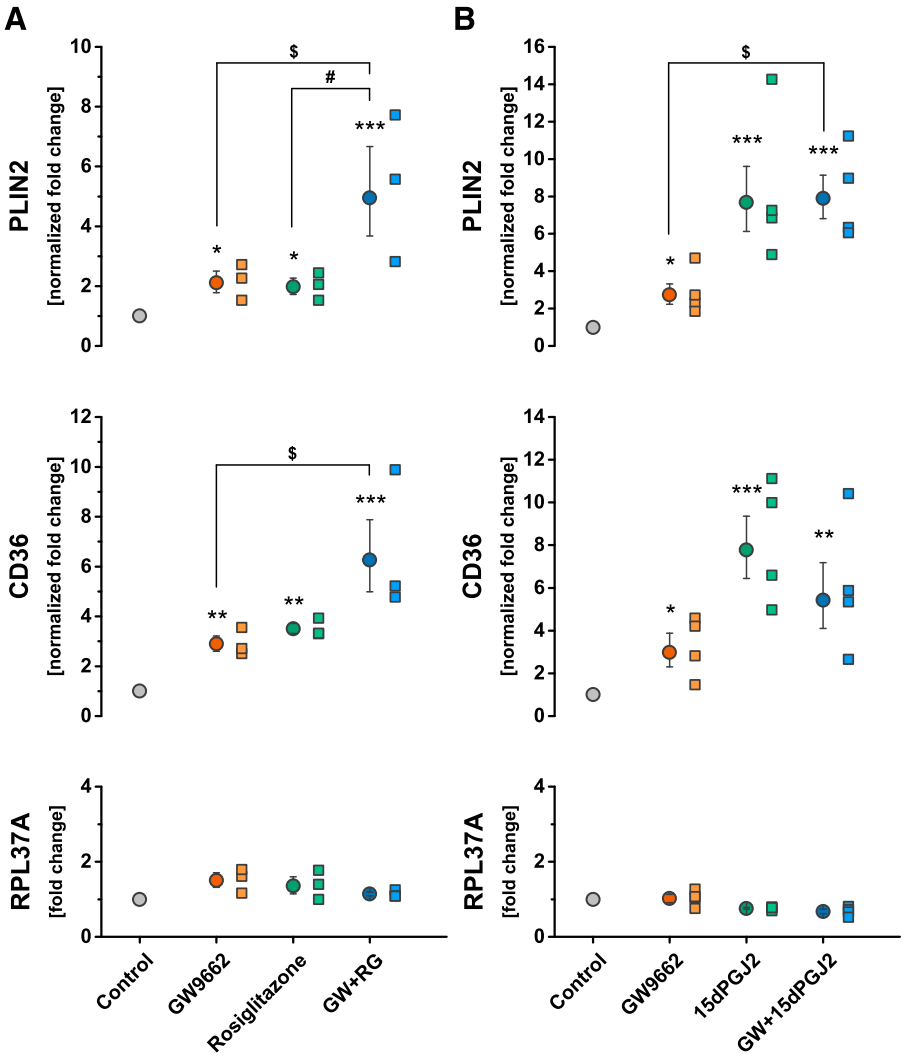

Fig. 1. GW9662 exhibits PPARγ agonist–like activity and fails to block PPARγ agonists in human THP-1 macrophages. (A) Mature THP-1 cells were either treated with 10 μM GW9662 (GW) or 5 μM rosiglitazone (RG) alone or were pretreated with 10 μM GW9662 for 1 hour and then incubated with 5 μM rosiglitazone for another 24 hours (GW+RG). (B) THP-1 macrophages were either treated with 10 μM GW9662 (GW) or 5 μM 15dPGJ2 alone or were pretreated with 10 μM GW9662 for 1 hour and then incubated with 5 μM 15dPGJ2 for another 24 hours (GW+15dPGJ2). Expression levels of PLIN2, CD36, and the reference gene RPL37A were assessed by RT-qPCR. Expression of the reference gene remained unchanged in both experimental setups and was used for normalization. GW9662 stimulated expression of PLIN2 and CD36 significantly. In combination with the PPARγ ligand rosiglitazone, GW9662 showed additive effects instead of blocking activity. Circles represent the mean of normalized fold changes of three (A) or four (B) independent biologic experiments. Error bars display calculated maximum and minimum expression levels based on the S.E.M. of ΔΔct values. Squares represent data of independent biologic experiments to visualize variability of the data. $^{*}P < 0.05$; $^{**}P < 0.01$; $^{***}P < 0.001$; all vs. control (0 μM GW9662); $^{\#}P < 0.05$ vs. PPARγ ligand only; $^{\$}P < 0.05$ vs. GW9662 only. P values were calculated using repeated-measures ANOVA with Tukey's post hoc test.

levels of PLIN2 mRNA (Supplemental Fig. 3). Having identified the unexpected property of GW9662 to stimulate the expression of known PPARγ target genes, we aimed at the characterization of this effect. This is of interest, as GW9662 is widely used in scientific studies that do not necessarily resemble our initial setup.

Concentration-Dependent Activation of PLIN2 Expression by GW9662. Concentration dependency was investigated to obtain further insights into the dynamics of the regulation of PLIN2 expression by GW9662. THP-1 cells were therefore treated with different concentrations of GW9662 for 24 hours, as indicated in Supplemental Fig. 4. Stimulation with a concentration of 1 μM GW9662 already significantly induced PLIN2 mRNA expression in THP-1 macrophages to the 2.2-fold compared with controls ($P < 0.001$). This effect was augmented further with increasing concentrations up to the 3.2-fold ($P < 0.001$ at 5–50 μM for 24 hours). These findings indicate that upregulation of PPARγ target genes is a robust effect in different experimental setups. However, we used GW9662 at a concentration of 10 μM for further experiments because this concentration revealed reproducible results and is a commonly used concentration in published scientific studies (Lea et al., 2004; Kourtidis et al., 2009). As GW9662 reliably induces PPARγ target genes and is thus not usable for blocking experiments, we were interested in the PPARγ antagonist 2-chloro-5-nitro-N-4-pyridinyl-benzamide (T0070907) (Lee et al., 2002) with inverse agonist properties (Lee et al., 2002; Brust et al., 2018) as an alternative. However, incubation with 1 μM T0070907 for 24 hours induced PLIN2 mRNA expression in THP-1 macrophages to the 1.4-fold compared with controls, and this induction increased with higher concentrations up to the 2.5-fold, as shown in Supplemental Fig. 5. Thus, T0070907 has similar effects as GW9662 on PLIN2 gene expression and is neither an alternative for GW9662 nor a useful tool to further characterize GW9662's effects in our setup.

PLIN2 mRNA Expression Is Induced by GW9662 in Human and Mouse Macrophages. Because GW9662 is often used to confirm PPARγ-mediated effects, and no comparable effects to our observations have been reported (to the best of our knowledge), we considered a THP-1 cell–specific "artifact" as possible explanation. Thus, we examined PLIN2 and CD36 mRNA expression in primary macrophages and in other macrophage cell lines of human and murine origin in response to GW9662. For these studies, we incubated different human macrophage cells (THP-1, U937, and primary macrophages) as well as different mouse macrophages (RAW264.7, J774A.1, and primary peritoneal macrophages) with 10 μM GW9662 for 24 hours in serum-free medium and compared expression of PLIN2/Plin2 and CD36/Cd36 with controls cultured in serum-free medium in the absence of GW9662. Except for RAW264.7 cells, GW9662 induced expression of PLIN2/Plin2 mRNA in every cell type investigated at least to the 1.9-fold, as shown in Fig. 2 (top; $P < 0.05$ for THP-1, U937, and J774.A1). In contrast, the effect of GW9662 on CD36/Cd36 mRNA expression was more inconsistent. Though expression of CD36/Cd36 mRNA tended to be increased in U937 cells and was significantly increased in THP-1 macrophages as well as

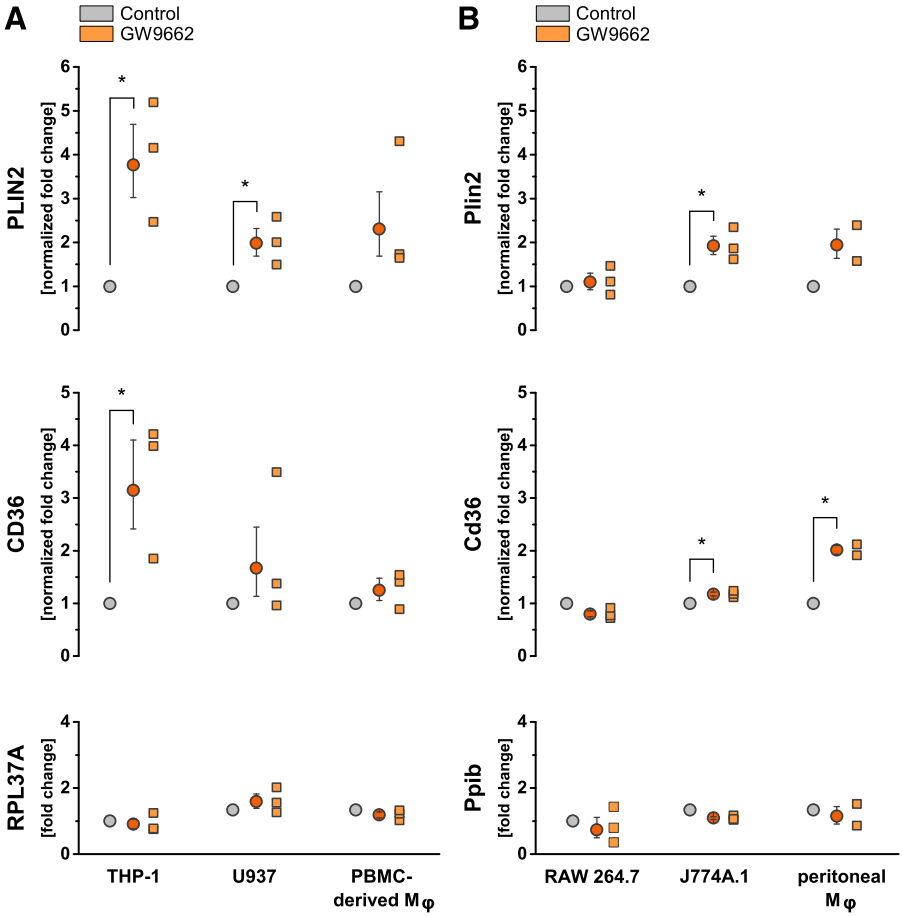

Fig. 2. GW9662 induces expression of PLIN2/Plin2 and CD36/Cd36 in different human and murine macrophage cell models. Human (A) and murine (B) macrophages of different origin were incubated with 10 μM GW9662 for 24 hours. Relative mRNA levels were measured by RT-qPCR and compared with control cells cultured in absence of GW9662. Gene expression levels of human cells were normalized to RPL37A; expression levels of murine cells were normalized to Ppib. Circles represent means of fold changes of three independent biologic replicates (except for peritoneal macrophages, for which independent experiments were performed twice). Squares represent the mean of two technical replicates of the biologic replicates. Error bars display calculated maximum and minimum expression levels based on the S.E.M. of ΔΔct values. *$P <$ 0.05 vs. corresponding control. P values were calculated using two-tailed paired t test.

in peritoneal macrophages and J774A.1 to the 3.2-fold ($P < 0.05$; Fig. 2A, middle), to the 2.0-fold ($P < 0.05$; Fig. 2B, middle), and to the 1.18-fold ($P < 0.05$), respectively, expression of CD36/Cd36 in human PBMCs and murine RAW264.7 was not affected. Expression of the reference genes RPL37A and Ppib remained unchanged in all experiments (Fig. 2, bottom). Consequently, the effect of GW9662 is not restricted to THP-1 cells but is also observed in other human and murine macrophage-like cells as well as in primary human macrophages and mouse peritoneal macrophages.

GW9662 Induces PLIN2 mRNA Consistently and Comparable to Synthetic and Natural PPARγ Agonists. To confirm that our observations do not depend on lot or supplier, GW9662 from two different distributors and in two lots of a single renowned distributor were tested. Consistently, PLIN2 mRNA expression was induced in mature THP-1 macrophages after treatment with 10 μM GW9662 for 24 hours in all cases. However, fold changes varied between experiments performed with GW9662 from different lots between about three- and sixfold (Supplemental Fig. 17). Most strikingly, in some experiments, the ability of GW9662 to induce PLIN2 mRNA and protein levels was comparable to that of the PPARγ agonists rosiglitazone and 15dPGJ2 (Fig. 3). In the case of CD36, GW9662 was almost as potent as 15dPGJ2 to induce CD36 mRNA expression but was less potent than rosiglitazone (Fig. 3A). However, as mentioned above, results for the impact of GW9662 on CD36 expression were inconsistent.

PLIN2 Protein Levels in THP-1 Macrophages Are Elevated by GW9662. Given the reliable induction of PLIN2 gene expression by GW9662 in different setups and different cell lines, we were interested whether this effect is mirrored on the protein level. This would point to further, likely more complex, changes in cellular functions by GW9662. Western blot analyses confirmed indeed that PLIN2 protein levels were significantly increased in THP-1 macrophages to about the 1.9-fold ($P < 0.05$) after 24 hours and to about the 1.4-fold ($P < 0.05$) after 48 hours of treatment with 10 μM GW9662 compared with the respective controls (Fig. 4, A and B). For immunoblotting, PLIN2 was evaluated densitometrically and normalized to α-tubulin. The expression of α-tubulin was not affected by GW9662 (Fig. 4A). Immunofluorescence staining further supports our notion that GW9662 significantly induced PLIN2 protein in THP-1 macrophages compared with nontreated controls ($P < 0.01$; Fig. 4, C and D). As with the effect of T0070907 on gene expression of PLIN2, we were interested if the alternative PPARγ antagonist exerts comparable effects to GW9662 on the protein level. Western blot

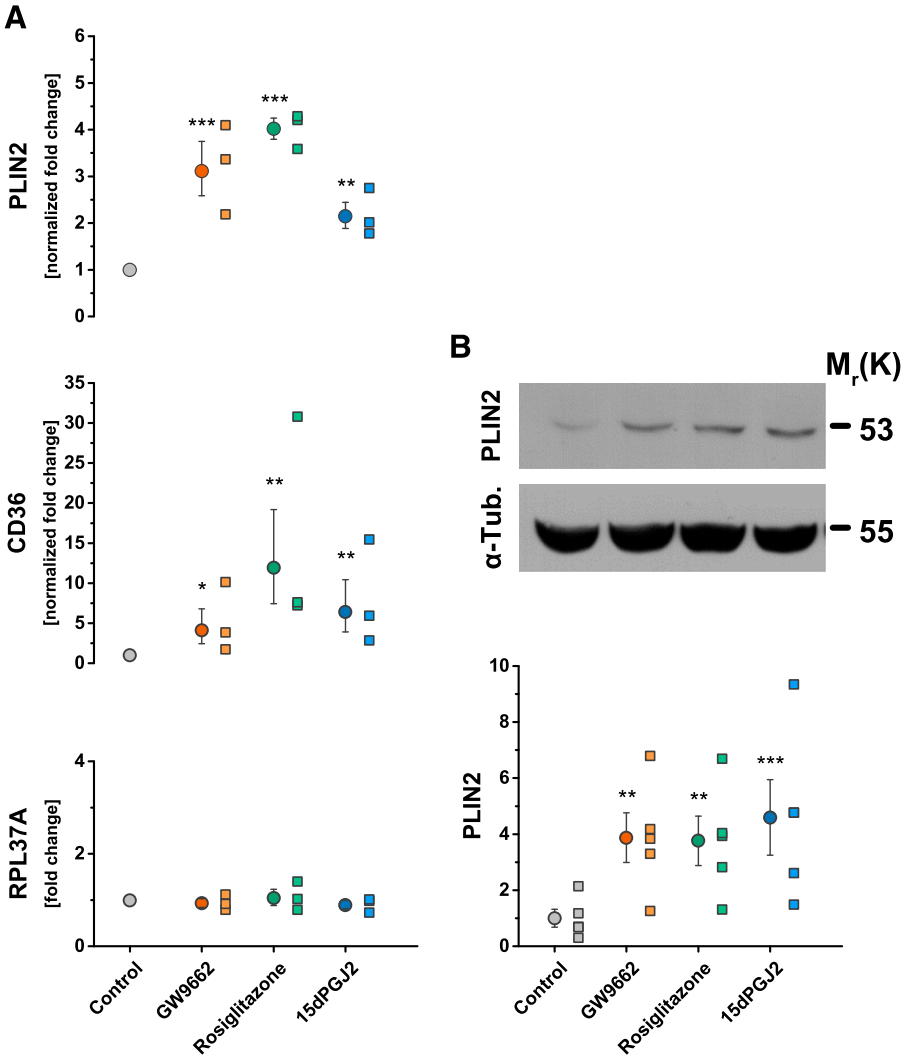

Fig. 3. GW9662 induces PLIN2 expression comparable to the PPARγ agonists rosiglitazone and 15dPGJ2. Mature THP-1 macrophages were treated with either vehicle (control), 10 μM GW9662 (GW), 5 μM rosiglitazone (RG), or 5 μM 15dPGJ2 for 24 hours. (A) PLIN2 and CD36 mRNA expression levels were assessed by RT-qPCR and normalized to the expression of RPL37A. Circles represent means of fold changes of three independent biologic replicates. Squares represent the mean of two technical replicates of the biologic replicates. Error bars display calculated maximum and minimum expression levels based on the S.E.M. of ΔΔct values. (B) Top: representative Western blot. Bottom: relative protein levels of PLIN2 as estimated by densitometric analysis of Western blots. Circles represent means of fold changes of five independent experiments. Squares represent means of two technical replicates of the biologic replicates relative to the mean of the control to visualize variability of the data. α-Tubulin (α-Tub.) was used as loading and cell viability control and was used for normalization. Data are shown as mean ± S.E.M. $*P < 0.05$; $**P < 0.01$; $***P < 0.001$ vs. control. P values were calculated using repeated-measures ANOVA with Dunnett's post hoc test vs. control as reference.

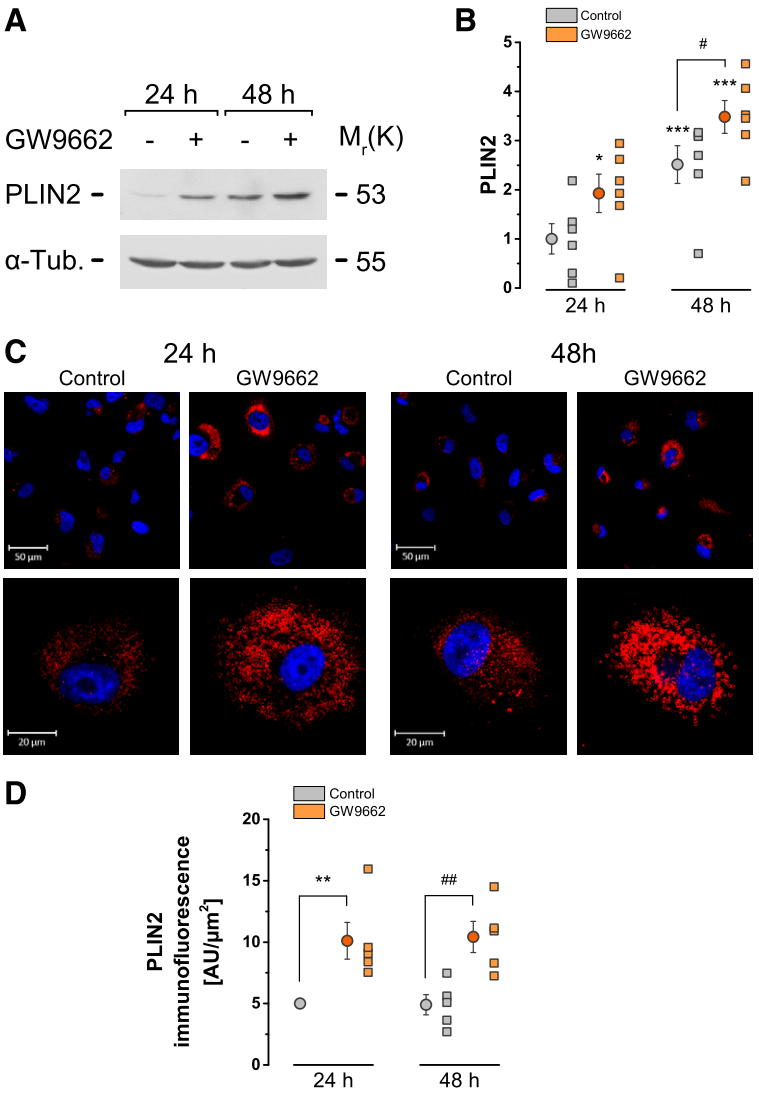

Fig. 4. GW9662 augments PLIN2 protein expression in mature THP-1 macrophages. PMA-matured THP-1 macrophages were cultured in presence or absence of 10 μM GW9662 for 24 and 48 hours. PLIN2 protein levels were assessed by Western blot analysis and immunofluorescence. (A) Representative Western blot of PLIN2 protein levels. α-Tubulin (α-Tub.) was used as loading and cell viability control. (B) Relative densitometric quantification of Western blot results. Circles represent means of fold changes of five independent experiments. Squares represent independent biologic replicates relative to the mean of the control to visualize variability of the data. (C) Immunofluorescence staining of PLIN2 and Hoechst Dye 33258 staining of nuclei. Representative cells are shown at magnifications as indicated. (D) Relative intensities of immunofluorescence signals per area shown as arbitrary units (AU/μm^2) × 10^4. Circles represent data of five independent experiments shown as mean ± S.E.M. Squares represent independent biologic replicates relative to the control to visualize variability of the data. $^*P < 0.05$; $^{**}P < 0.01$; $^{***}P < 0.001$ vs. 24-hour control; $^{\#}P < 0.05$; $^{\#\#}P < 0.01$ vs. 48-hour control. *P* values were calculated using repeated-measures ANOVA with Tukey's post hoc test.

analyses confirmed that PLIN2 protein levels were slightly increased in THP-1 macrophages after 24 and 48 hours of treatment with 10 μM T0070907 (Supplemental Fig. 6). Thus, T0070907 apparently exerts less unwanted effects on the protein level and might be a usable alternative to GW9662 in some experimental setups.

GW9662 Affects Expression of Several Other PPAR Target Genes. Because we demonstrated that GW9662 unexpectedly induces the expression of PLIN2 and CD36 mRNA (as well as PLIN2 protein), we were interested in whether and how GW9662 affects the expression of other PPAR target genes. For this purpose, we used Lonza Human PPAR Signaling 384 StellARray qPCR arrays. These arrays allow the measurement of the expression of 384 genes that are either regulated by the PPAR subtypes (PPARα, PPARβ/δ, and PPARγ) themselves, are PPAR-interacting partners, or serve as controls (HsGenomic and Hs18s) and reference genes (nine most stably expressed genes).

For profiling analyses, THP-1 macrophages were treated for 24 hours either with solvent only as control or 10 μM GW9662. Samples obtained from five independent experiments were pooled in equal proportions, and relative changes in expression were measured using RT-qPCR. Results were normalized to the nine most stably expressed reference genes as selected by the Lonza Global Pattern Recognition algorithm. Genes were grouped according to their regulation into "upregulated," "downregulated," and "unchanged" (Supplemental Table 4). For this, a fold change of 1.5 was set as the cutoff as recommended by the supplier. Genes that were not detected are listed separately as "not expressed/not detectable" (Supplemental Table 3). As shown in Supplemental Fig. 7A, expression of most of the genes (47.4%) remained unchanged by GW9662, whereas expression was upregulated for 26.6% and downregulated for 16.9% of the genes. For 9.1% of the genes, no expression was detectable.

As illustrated in Supplemental Fig. 7B, most of the genes with expression altered by GW9662 in THP-1 macrophages are involved in lipid and glucose metabolism, immune and inflammatory response, and signal transduction and transcription. In more detail (Supplemental Fig. 8), genes affected by GW9662 are involved in: 1) glucose transport, such as sorbin and SH3 domain containing 1, protein phosphatase 2α, and insulin receptor; 2) in glycolysis, such as pyruvate dehydrogenase kinase 4; 3) lipid uptake, such as CD36, oxidized low-density lipoprotein receptor 1, and low-density lipoprotein receptor; 4) lipid transport, such as fatty acid transport

members 1 and 2 of the solute carrier family 27, and FABP2 to FABP4; 5) lipid storage, such as PLIN2; and 6) lipogenesis, such as stearoyl-CoA desaturase, acetyl-coenzyme A carboxylase α, and members 3–5 of the acyl-CoA synthetase long-chain family. Furthermore, proinflammatory genes, such as cytosolic phospholipase A_2, interleukin 1β, prostaglandin E receptor 2, and inducible nitric oxide synthase 2, are also induced by GW9662.

The results of the array nicely show that the effects of GW9662 go far beyond the initially observed regulation of PLIN2 and CD36. Interestingly, these genes are members of the most affected functional category, the lipid metabolism. Taken together, GW9662 influences genes in all classic PPAR-related metabolic pathways (lipid metabolism, glucose metabolism, immunity, and inflammation) (Clark, 2002; Wang, 2010). This indicates that use of GW9662 affects cellular metabolism in different ways, and thus applicability of GW9662 should be carefully evaluated in different experimental setups.

GW9662 Induces Triglyceride Accumulation in THP-1 Macrophages. According to the expression profiling, GW9662 regulates a variety of genes implicated in lipid metabolism. We were therefore interested in if subsequent functional consequences occur. The choice of an appropriate readout was based on our finding that PLIN2 is regulated at the protein level by GW9662. PLIN2 has been shown to be involved in the import and storage of cholesterol and fatty acids (Paul et al., 2008). Together with the observation that more lipid droplet-like structures appear in GW9662-treated THP-1 macrophages compared with controls, we decided to investigate whether GW9662 induces the accumulation of lipids, particularly triglycerides. Therefore, we analyzed the intracellular content of triglycerides and total cholesterol. In good agreement with our findings reported above, 10 μM GW9662 increased triglyceride levels in THP-1 macrophage cells by 27% compared with control after 24 hours ($P < 0.01$). However, after 48 hours, no significant effect compared with the respective control was observed (Fig. 5, left). In contrast, the total cellular cholesterol content was not altered by GW9662 after 24 or 48 hours (Fig. 5, right).

GW9662 Raises Lipogenesis in THP-1 Macrophages. The expression profiling revealed that several genes implicated in lipogenesis are upregulated by GW9662. Therefore, we analyzed lipogenesis in THP-1 macrophages to gain deeper insight into the molecular causes for the increased intracellular total triglyceride content. Mature macrophages were incubated with 10 μM GW9662 for 24 hours and with ^{14}C-acetate for 4 hours. We found a 34% increased incorporation of ^{14}C-acetate ($P < 0.001$) compared with controls cultured in the absence of GW9662 (Fig. 6). As a negative control, C75, an inhibitor of fatty acid synthesis, was used at concentrations of 50 or 100 μM for 6 hours. C75 inhibited ^{14}C-acetate incorporation to approximately 70% of control (Supplemental Fig. 15). The findings are in good agreement with the observed increased intracellular triglyceride content by GW9662 (Fig. 5) and the results obtained from mRNA expression analyses using Lonza Human PPAR Signaling 384 StellARray qPCR arrays (Supplemental Table 3 and Supplemental Figs. 7–9). Taken together, GW9662 treatment leads to substantial changes in macrophage lipid metabolism, as shown by alterations in gene regulation leading to higher levels of lipid synthesis and storage in consequence.

PPARδ Mediates the Effects of GW9662 on PLIN2 and CD36 Expression in THP-1 Macrophages. The treatment of THP-1 macrophages with GW9662 leads to substantial changes in cellular metabolism, particularly in lipid metabolism. Thus, the underlying mechanism of action is of special interest to assess the applicability of GW9662 in certain experimental setups. Previous studies using GW9662 revealed that this compound is not entirely specific for PPARγ (Leesnitzer et al., 2002). Hence, the interaction of GW9662 with other PPAR subtypes or nuclear receptors is a possible reason for the unexpected effects reported here. To reveal a possible role of the distinct PPAR subtypes in the observed regulation of PLIN2 and CD36, siRNA was used to knock down each PPAR subtype in THP-1 macrophages. For this purpose, THP-1 monocytes were differentiated for 24 hours using PMA. Resulting THP-1 macrophages were transfected with either negative control siRNA or siRNA for each PPAR subtype and transfection efficiency was verified (Supplemental Fig. 14). The macrophages were allowed to recover for 72 hours and were then incubated with 10 μM GW9662 or vehicle for 24 hours. The expression of PLIN2 and CD36 was induced by GW9662 in all transfected cells. However, the extent of the induction of PLIN2 and CD36 expression by GW9662 was significantly lowered in the PPARδ-depleted cells. PLIN2 was merely induced to the 2.5-fold compared with the respective control in PPARδ-depleted cells, whereas an increase to the 4.7-fold in cells transfected with negative control siRNA or with PPARα siRNA and an increase to the 4.2-fold over the respective control was observed in PPARγ-depleted cells (Fig. 7). Similarly, CD36 expression was induced only to the 1.8-fold by GW9662 in PPARδ-depleted cells but to the 2.7-, 2.8-, and 3.7-fold in

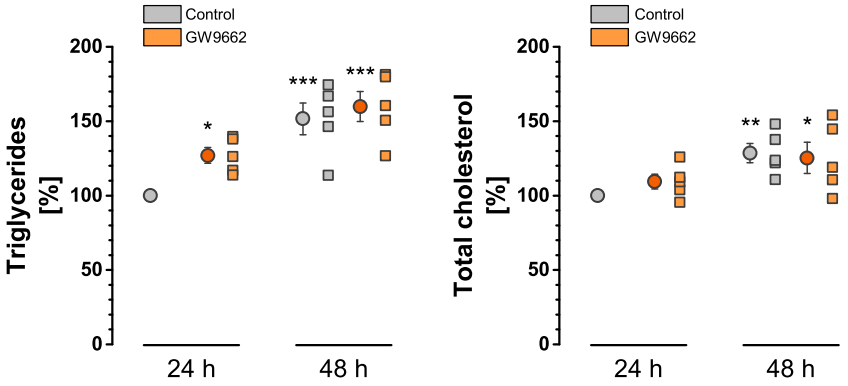

Fig. 5. GW9662 promotes intracellular accumulation of triglycerides but not of total cholesterol. Differentiated THP-1 cells were treated with 10 μM GW9662 in lipid- and serum-free medium for 24 and 48 hours. Cells cultured in absence of GW9662 served as controls. Triglyceride or total cholesterol levels in untreated 24-hour controls were arbitrarily set to 100%. Circles represent mean ± S.E.M. of five independent experiments. Squares represent independent biologic replicates relative to the control to visualize variability of the data. *$P < 0.05$; **$P < 0.01$; ***$P < 0.001$. In both cases, P values are provided for GW9662 vs. control after 24 hours. P values were calculated using repeated-measures ANOVA with Tukey's post hoc test.

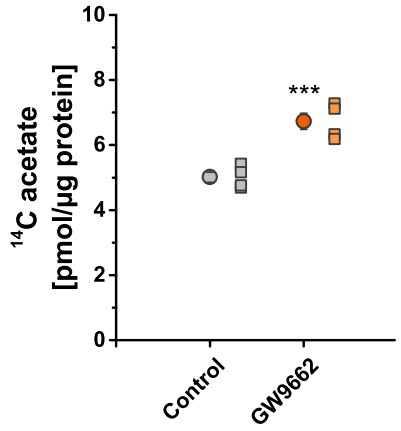

Fig. 6. GW9662 stimulates lipogenesis in THP-1 macrophages. Mature THP-1 macrophages were treated with 10 μM GW9662 for 24 hours in serum-free medium. After 20 hours, ^{14}C-acetate was added for the next 4 hours. Samples were processed, and ^{14}C-radioactivity was measured by scintillation. Incorporated ^{14}C-acetate was normalized to cellular total protein content. Circles represent mean ± S.E.M. of four independent experiments. Squares represent independent biologic replicates relative to the control to visualize variability of the data. ***$P < 0.001$. The P value is provided for GW9662 vs. control, calculated using two-tailed paired t test.

control cells transfected with negative control siRNA, PPARα, or PPARγ knockdown, respectively (Fig. 7). Thus, PPARδ knockdown significantly impairs the effect of GW9662 on PLIN2 ($P < 0.05$) and CD36 ($P < 0.05$; $P < 0.0565$ for negative control siRNA) expression in THP-1 macrophages.

The knockdown experiments provide evidence that PPARδ is involved in the effects of GW9662 on PLIN2 and CD36 expression. However, PPARδ knockdown did not completely abolish the induction of target genes by GW9662. Thus, there might be remaining activity of PPARδ or further regulatory proteins that might be affected by GW9662. However, to verify the contribution of PPARδ to the effects of GW9662, a chemical antagonist was used to block PPARδ activation. Mature THP-1 macrophages were therefore preincubated with 1 μM of the PPARδ antagonist GSK3787 (Shearer et al., 2010) for 1 hour, and GW9662 was added for an additional 24 hours. Furthermore, cells were treated with GSK3787 or GW9662 alone for 24 hours. The PPARδ antagonist GSK3787 itself induced PLIN2 expression to the 1.5-fold. As expected, GW9662 induced PLIN2 expression to the threefold. Preincubation with GSK3787 completely abolished the effect of GW9662, as the induction to the 1.4-fold over control shows (Fig. 8). Similarly, GSK3787 induced CD36 expression to the 1.8-fold, whereas GW9662 induced the expression to the 1.4-fold; in combination, merely an induction to the 1.5-fold was found (Fig. 8). Taken together, we provide convincing evidence that the unexpected effects of GW9662 on the expression of the PPAR target genes PLIN2 and CD36 are mediated at least in part by the ability of GW9662 to directly or indirectly activate PPARδ.

Discussion

We identified PPARδ as mediator of the unexpected effects of the well-known PPARγ antagonist GW9662 on lipid metabolism in human and murine macrophages. The off-target action of GW9662 was confirmed in pharmacological antagonist experiments as well as in studies with siRNA-mediated knockdown of PPARδ. The awareness of the PPARδ-activating properties of GW9662 requires a reinterpretation of results obtained using GW9662 in previous studies.

Initially, we used GW9662 with the intention to show the reported regulatory function of PPARγ on PLIN2 (Buechler et al., 2001; Fan et al., 2009) and CD36 (Chawla et al., 2001; Moore et al., 2001; Tontonoz et al., 1998) expression in macrophages. Surprisingly, GW9662 induced the expression of these genes comparable to synthetic (rosiglitazone) and natural (15dPGJ2) PPARγ agonists (Figs. 1 and 3). Moreover,

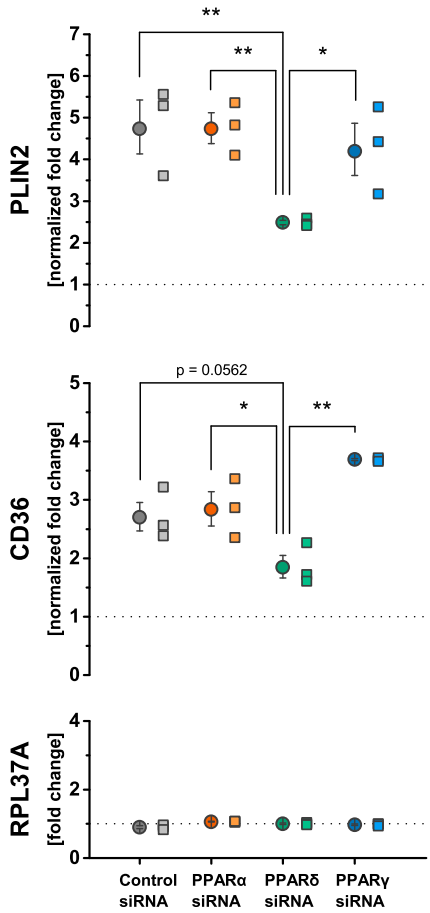

Fig. 7. siRNA-mediated PPARδ knockdown diminishes PLIN2 and CD36 induction by GW9662 in THP-1 macrophages. THP-1 monocytes were differentiated with PMA for 24 hours. Premature THP-1 cells were transfected with siRNA for the indicated PPAR subtypes or an appropriate negative control siRNA. The cells could recover for 72 hours. Then, cells were either treated with 10 μM GW9662 or vehicle (control) for 24 hours. Expression levels of PLIN2, CD36, and the reference gene RPL37A were assessed by RT-qPCR. Expression of the reference gene remained unchanged in the experimental setup and was used for normalization. Data are presented as fold change of treatment (GW9662) vs. the respective control (vehicle) in cells transfected with the indicated siRNAs. Vehicle controls were set to 1 and are represented by the dotted line. GW9662 induced the expression of PLIN2 and CD36 compared with the respective control, irrespective of the targeted PPAR subtype. The extent of PLIN2 and CD36 induction compared with the respective control is significantly lower in cells with PPARδ knockdown than with PPARα or PPARγ knockdown or the negative control siRNA. Circles represent the mean of normalized fold changes of three independent biologic experiments. Error bars display calculated maximum and minimum expression levels based on the S.E.M. of ΔΔct values. Squares represent the mean of two technical replicates of the biologic replicates. *$P < 0.05$; **$P < 0.01$; GW9662 treatment vs. GW9662 treatment and PPARδ knockdown. P values were calculated using one-way ANOVA with Tukey's post hoc test.

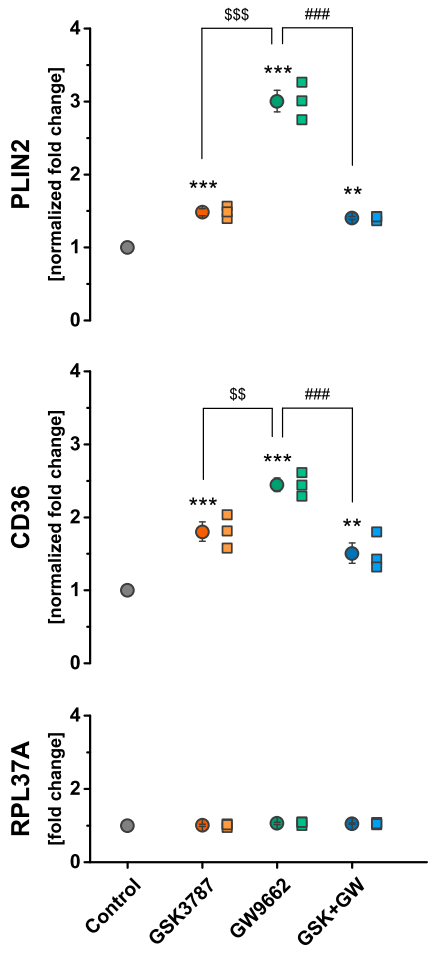

Fig. 8. PPARδ antagonist GSK3787 blocks PLIN2 and CD36 induction by GW9662 in THP-1 macrophages. Mature THP-1 cells were either treated with 10 μM GW9662 or 1 μM GSK3787 without pretreatment for 24 hours or pretreated with GSK3787 for 1 hour and then incubated with 10 μM GW9662 (GSK+GW) for another 24 hours. Expression levels of PLIN2, CD36, and the reference gene RPL37A were assessed by RT-qPCR. Expression of the reference gene remained unchanged in the experimental setup and was used for normalization. Treatment with GSK3787 or GW9662 alone significantly induced the expression of PLIN2 and CD36. In combination, GSK3787 blocks the induction of PLIN2 and CD36 by GW9662. Circles represent the mean of normalized fold changes of three independent biologic experiments. Error bars display calculated maximum and minimum expression levels based on the S.E.M. of ΔΔct values. Squares represent the mean of two technical replicates of the biologic replicates. $^{**}P < 0.01$; $^{***}P < 0.001$; all vs. control (0 μM GSK3787/GW9662); $^{\#\#\#}P < 0.001$; GSK+GW vs. GW9662 only; $^{\$\$}P < 0.01$; $^{\$\$\$}P < 0.001$; GW vs. GSK3787. *P* values were calculated using repeated-measures ANOVA with Tukey's post hoc test.

the combination of GW9662 with rosiglitazone even enhanced target gene expression (Fig. 1A), indicating a rather unlikely PPARγ-activating property of GW9662 or the activation of one or more PPARγ-independent signaling pathways. Therefore, GW9662 is not usable to elucidate PPARγ-mediated effects in macrophages. This observation leads to the question about the causes for the unexpected, even opposite, action of the accepted and frequently used PPARγ antagonist GW9662 in macrophages.

To address this question, known properties of the PPAR family were taken into consideration. The affinity of the PPAR subtypes for ligands is thought to be mainly determined by the size of the ligand-binding pocket (Bugge and Mandrup, 2010). Consequently, small molecules like GW9662 potentially bind to all PPAR subtypes. Furthermore, the DNA-binding domains of the PPAR subtypes show a high structural and sequence homology (Escher and Wahli, 2000); thus, most PPAR target genes are regulated by all three subtypes. Based on this, we performed combinatory experiments with synthetic PPARα and PPARδ antagonists. The PPARδ antagonist GSK3787 completely abolished the induction of PLIN2 and CD36 gene expression by GW9662 (Fig. 8), whereas the PPARα antagonist GW6471 did not (Supplemental Fig. 10). Moreover, we verified the contribution of PPARδ but not PPARα or PPARγ to the effects of GW9662 via siRNA-mediated knockdown of the PPAR subtypes (Fig. 7). These findings are in line with studies reporting the contribution of PPARδ to PLIN2 (Chawla et al., 2003; Fan et al., 2009) and CD36 (Li et al., 2004; Bojic et al., 2012) expression.

The proposed ability of GW9662 to bind to all PPAR subtypes (vide supra) has indeed been shown. Although GW9662 was identified as a potent antagonist of PPARγ, it also covalently modifies PPARα and PPARδ at higher concentrations (Leesnitzer et al., 2002). Notwithstanding the differences in the affinity of GW9662, the effects observed in this study are mediated by PPARδ. This is likely reasoned by the abundant expression of PPARδ, a hallmark of THP-1 cell differentiation (Vosper et al., 2001) (Supplemental Fig. 16). The resulting predominance of PPARδ in THP-1–derived macrophages (as well as in the other macrophage cell lines in this study; Supplemental Table 6) likely favors the effects of GW9662 via PPARδ over PPARγ and PPARα. This assumption is supported by the fact that differential tissue distribution is one main factor of subtype-specific effects of PPARs (Bugge and Mandrup, 2010). Concerning subtype distribution in macrophages, no effect of GW9662 treatment was observed (Supplemental Fig. 11). The induction of PPAR target genes by GW9662 as well as the blocking by a PPARδ antagonist suggests that GW9662 acts predominantly as a PPARδ agonist in macrophages. Contradictory to this, GW9662 has initially been characterized as an antagonist of PPARδ using an assay based on a fusion protein containing the ligand binding domain of PPARδ and the galactose-responsive transcription factor 4 (Leesnitzer et al., 2002) and was later confirmed with a similar approach (Leesnitzer et al., 2002; Seimandi et al., 2005). Interestingly, the authors of the initial study were not able to confirm the PPARδ antagonism in an assay based on the full-length receptor and a luciferase reporter. Here, even an activation of PPARδ was observed (Leesnitzer et al., 2002), indicating that GW9662 is indeed able to activate gene expression via PPARδ in "native" cellular systems like THP-1 macrophages. A recent report supports the notion of different effects in artificial and "native" systems (Brust et al., 2018). Though GW9662 shows no effect in a cell-based full-length PPARγ luciferase assay, the expression of the PPARγ target genes FABP4 and CD36 tends to be increased by GW9662 in "native" adipocyte-like cells (Brust et al., 2018). In line with these findings, GW9662 acted as a reliable inducer of PLIN2 gene expression even in low concentrations (1 μM) in our hands (Supplemental Fig. 4). Summarizing the above delineated results, we propose that GW9662 directly activates PPARδ in macrophages but do not prove this interaction experimentally. Thus, based on our data, we cannot completely rule out that GW9662 induces a signaling cascade that finally leads to PPARδ activation. In this context, the increased production of endogenous PPARδ

ligands via the cyclooxygenase (COX) pathway (Gupta et al., 2000) is unlikely, as GW9662 does not affect gene expression of COX1 and COX2 (Supplemental Fig. 12B). However, the elucidation of a potential signaling pathway indirectly activating PPARδ goes beyond the scope of this single work.

Notwithstanding that the mechanism of PPARδ activation by GW9662 is not fully elucidated, our data convincingly demonstrate that GW9662 causes notable effects in macrophage cell models and may thus provoke erroneous interpretation of experimental data (especially with respect to the contribution of PPARγ). Administration of GW9662 to macrophages leads to remarkable changes in the expression of PPAR target genes. About 44% of the target genes included in our profiling were regulated. This profiling analysis allows the attribution of these genes to PPAR subtypes (Supplemental Table 4). However, an unambiguous assignment is not possible. The expression of PPAR target genes is undoubtedly dependent on the differential expression of the PPAR subtypes in cells as well as the "setting" of the target sites like chromatin modification and the combination of other transcription factors, which is highly cell-type specific (Nielsen et al., 2006).

For this reason, the expression profiling data should be interpreted as PPAR-mediated effects in general rather than subtype-specific effects. Given the identification of PPARδ as mediator of PLIN2 and CD36 regulation, most of the genes in the array are likely also regulated via activation of PPARδ by GW9662. Although the predominance of PPARδ in THP-1 macrophages supports this assumption, we cannot give final proof. However, there are substantial changes in PPAR target gene expression induced by GW9662. These genes are involved in immunity and inflammation, signal transduction and transcription, and glucose metabolism and, particularly, lipid metabolism (Supplemental Table 5; Supplemental Fig. 7). More than half of the genes implicated in lipid metabolism included in the array were regulated by GW9662. In addition to PLIN2 (lipid storage) and CD36 (lipid import), other genes involved in the import, transport, storage, and export of lipids as well as β-oxidation and lipogenesis are affected. Most of the upregulated genes can be assigned to lipid import, lipid transport, and lipogenesis (Supplemental Fig. 8). Consequently, accumulation of fatty acids, and thus their storage form triglycerides, in the cell caused by GW9662 can be expected. In particular, the upregulation of acetyl-coenzyme A carboxylase-α as the rate-limiting enzyme in fatty acid synthesis (Tong and Harwood, 2006) is noteworthy. This enzyme catalyzes the carboxylation of acetyl-CoA to malonyl-CoA, which is not only a substrate for fatty acid biosynthesis but is also known to suppress β-oxidation (Tong and Harwood, 2006). Thus, synthesis and storage of fatty acids is more likely than degradation. Indeed, we have shown that GW9662 enhances lipogenesis from ^{14}C-acetate in THP-1 macrophages (Fig. 6). The increased lipogenesis necessitates the storage (or export) of the resulting free fatty acids to prevent potential harmful lipotoxic effects. Macrophages treated with GW9662 showed an augmented triglyceride content, suggesting that enhanced lipogenesis indeed causes fatty acid synthesis and storage in the form of triglycerides (Fig. 5). This finding is in line with earlier reports from breast cancer cells. GW9662 causes triglyceride accumulation in T47D cells (Lea et al., 2004) as well as BT474 and MCF-7 cells (Kourtidis et al., 2009). In the latter two cell lines, total fat and triglyceride stores were increased by GW9662 treatment. The higher lipid levels in BT474 cells are primarily caused by an increase in palmitic and stearic acid (Kourtidis et al., 2009). This indicates a higher rate of fatty acid synthesis, which is in line with our observations in the THP-1 cell model. Furthermore, GW9662 downregulates hormone-sensitive lipase and patatin-like phospholipase domain containing 2 in BT474 cells, the major enzymes in intracellular triglyceride breakdown (Kourtidis et al., 2009). However, patatin-like phospholipase domain containing 2 remained unaffected, whereas hormone-sensitive lipase was upregulated in our expression profiling (Supplemental Table 3) but was downregulated in confirmatory RT-qPCR experiments (Supplemental Fig. 12A) in GW9662-treated THP-1 cells. Taken together, though augmented lipid import can be excluded (serum-free conditions), the reduced triglyceride breakdown might also contribute to triglyceride accumulation, but the main cause is likely the increase in lipogenesis by GW9662.

Given that GW9662 regulates PLIN2 and CD36 via PPARδ, the observed effects on lipogenesis and triglyceride accumulation in response to GW9662 (Figs. 5 and 6) might be a global consequence of the activation of PPARδ. In contrast to this assumption, PPARδ is known for the stimulation of fatty acid oxidation in different tissues such as adipose tissue and skeletal muscles (Reilly and Lee, 2008). However, the role of PPARδ in lipid metabolism of macrophages is insufficiently characterized, and results of studies on this topic are inconsistent. PPARδ apparently exerts different effects on lipid metabolism and thus is not invariably a stimulator of lipid catabolism. For example, very low-density lipoprotein (VLDL) even stimulates triglyceride accumulation via activation of PPARδ in macrophages (Chawla et al., 2003; Bojic et al., 2012). Interestingly, pretreatment with PPARδ agonists attenuates VLDL-induced triglyceride accumulation by indirect inhibition of lipoprotein lipase (Bojic et al., 2012). In addition, fatty acid import via CD36 is upregulated (Li et al., 2004; Bojic et al., 2012), and β-oxidation of fatty acids is stimulated (Lee et al., 2006; Bojic et al., 2012) via PPARδ. Collectively, these mechanisms result in lower triglyceride accumulation in cells treated with PPARδ agonists than the THP-1 cells that are faced with VLDL alone (Bojic et al., 2012). However, the main factor might be the inhibition of VLDL triglyceride hydrolysis and not the β-oxidation of fatty acids; thus, lowering triglyceride accumulation in this setup would not be in contrast to our findings. Interestingly, both VLDL and PPARδ agonists as well as their combination induce expression of PLIN2 (Chawla et al., 2003; Bojic et al., 2012), which is known to stimulate triglyceride storage and synthesis in macrophages and inhibits β-oxidation (Larigauderie et al., 2006), contrasting the abovementioned results. Thus, PPARδ possibly acts as a switch; moderate activation of PPARδ (e.g., by VLDL or a PPARδ agonist) might favor lipid storage, whereas excessive PPARδ activation could shift the metabolism to lipid catabolism, likely to prevent lipid overload. Furthermore, PPARδ selectively responds to different "stimuli" of lipid metabolism; VLDL reliably activates PPARδ (Chawla et al., 2003; Lee et al., 2006; Bojic et al., 2012), whereas high-density lipoprotein and low-density lipoprotein do not (Chawla et al., 2003). The relationship of oxidized low-density lipoprotein and PPARδ is not clear (Vosper et al., 2001; Chawla et al., 2003; Li et al., 2004). As GW9662 induces PLIN2 and CD36 only

moderately and no additional stimuli were used, we expect moderate activation of PPARδ. This might lead to a "lipid storage" scenario in THP-1 macrophages in our hands. As we did not use any lipoproteins as stimulus, the studies of Vosper et al. (2001) on PPARδ and lipid accumulation in macrophages most accurately resemble our experimental setup. In line with our findings, the treatment with a PPARδ agonist upregulated the expression of genes involved in lipid metabolism, including CD36 and PLIN2, in this study. Consequently, the PPARδ activation promotes lipid accumulation in THP-1 macrophages in the presence of serum (Vosper et al., 2001). Taken together, the sparse data available on PPARδ and lipid accumulation in macrophages are in agreement with our finding that GW9662 promotes lipid accumulation via activation of PPARδ and consequent induction of genes involved in lipid metabolism, such as PLIN2 and CD36.

Conclusion

The widely used PPARγ antagonist GW9662 is unsuitable for the investigation of PPARγ signaling in human and murine macrophages because of its prominent off-target effects, likely occurring via PPARδ activation. Moreover, GW9662 itself induces expression of target genes that have been linked to PPARγ, such as PLIN2 and CD36, rather than blocking it. The induction of several additional genes by GW9662 leads to notable alterations in cellular metabolism, especially lipid metabolism, manifested as augmented lipogenesis and triglyceride accumulation. Thus, data obtained with GW9662 might lead to misinterpretation, particularly in macrophages and regarding lipid metabolism. Based on our findings, PPAR subtype expression of the used cell line should be considered when GW9662 is applied. Furthermore, the structurally related antagonist or inverse agonist T0070907 (Lee et al., 2002; Hughes et al., 2014; Brust et al., 2018) might be a useful alternative depending on the experimental setup (Supplemental Fig. 13), as we observed similar effects to GW9662 on RNA but not necessarily on the protein level. However, siRNA-mediated knockdown of PPARγ or PPARγ-deficient cells should be used in addition to PPARγ antagonists to confirm PPARγ-dependent regulatory effects. Considering the relevance of PPARs as therapeutic targets, the collection of reliable data is essential to draw appropriate conclusions. In this regard, our work will help to accurately interpret existing studies with GW9662 and to better design future studies.

Acknowledgments

We are grateful to Maria Braun, Silke Nossmann, and Thomas Böking for their excellent technical assistance. We thank Deutsche Forschungsgemeinschaft (DFG; RTG 1715), Deutsche Infarktforschungshilfe, Ernest-Solvay-Stiftung, Thüringer Ministerium für Bildung, Wissenschaft und Kultur, and Stiftung für Technologie und Forschung Thüringen for financial support to Stefan Lorkowski.

Authorship Contributions

Participated in research design: Schubert, Becher, Heller, Grün, Lorkowski.

Conducted experiments: Schubert, Becher, Wallert, Maeß, Große.

Contributed new reagents or analytic tools: Rennert, Mosig, Heller, Grün, Lorkowski.

Performed data analysis: Schubert, Becher, Wallert, Maeß, Abhari, Rennert, Große, Heller.

Wrote or contributed to the writing of the manuscript: Schubert, Becher, Mosig, Grün, Lorkowski.

References

Bickel PE, Tansey JT, and Welte MA (2009) PAT proteins, an ancient family of lipid droplet proteins that regulate cellular lipid stores. *Biochim Biophys Acta* **1791**: 419–440.

Bojic LA, Sawyez CG, Telford DE, Edwards JY, Hegele RA, and Huff MW (2012) Activation of peroxisome proliferator-activated receptor δ inhibits human macrophage foam cell formation and the inflammatory response induced by very low-density lipoprotein. *Arterioscler Thromb Vasc Biol* **32**:2919–2928.

Brunmeir R and Xu F (2018) Functional regulation of PPARs through post-translational modifications. *Int J Mol Sci* **19**:E1738.

Brust R, Shang J, Fuhrmann J, Mosure SA, Bass J, Cano A, Heidari Z, Chrisman IM, Nemetchek MD, Blayo A-L, et al. (2018) A structural mechanism for directing corepressor-selective inverse agonism of PPARγ. *Nat Commun* **9**:4687.

Buechler C, Ritter M, Duong CQ, Orso E, Kapinsky M, and Schmitz G (2001) Adipophilin is a sensitive marker for lipid loading in human blood monocytes. *Biochim Biophys Acta* **1532**:97–104.

Buers I, Robenek H, Lorkowski S, Nitschke Y, Severs NJ, and Hofnagel O (2009) TIP47, a lipid cargo protein involved in macrophage triglyceride metabolism. *Arterioscler Thromb Vasc Biol* **29**:767–773.

Bugge A and Mandrup S (2010) Molecular mechanisms and genome-wide aspects of PPAR subtype specific transactivation. *PPAR Res* **2010** DOI: 10.1155/2010/169506.

Chawla A, Barak Y, Nagy L, Liao D, Tontonoz P, and Evans RM (2001) PPAR-gamma dependent and independent effects on macrophage-gene expression in lipid metabolism and inflammation. *Nat Med* **7**:48–52.

Chawla A, Lee C-H, Barak Y, He W, Rosenfeld J, Liao D, Han J, Kang H, and Evans RM (2003) PPARdelta is a very low-density lipoprotein sensor in macrophages. *Proc Natl Acad Sci USA* **100**:1268–1273.

Clark RB (2002) The role of PPARs in inflammation and immunity. *J Leukoc Biol* **71**: 388–400.

Escher P and Wahli W (2000) Peroxisome proliferator-activated receptors: insight into multiple cellular functions. *Mutat Res* **448**:121–138.

Fan B, Ikuyama S, Gu J-Q, Wei P, Oyama J, Inoguchi T, and Nishimura J (2009) Oleic acid-induced ADRP expression requires both AP-1 and PPAR response elements, and is reduced by Pycnogenol through mRNA degradation in NMuLi liver cells. *Am J Physiol Endocrinol Metab* **297**:E112–E123.

Gruen M, Bommert K, and Bargou RC (2004) T-cell-mediated lysis of B cells induced by a CD19xCD3 bispecific single-chain antibody is perforin dependent and death receptor independent. *Cancer Immunol Immunother* **53**:625–632.

Gupta RA, Brockman JA, Sarraf P, Willson TM, and DuBois RN (2001) Target genes of peroxisome proliferator-activated receptor gamma in colorectal cancer cells. *J Biol Chem* **276**:29681–29687.

Gupta RA, Tan J, Krause WF, Geraci MW, Willson TM, Dey SK, and DuBois RN (2000) Prostacyclin-mediated activation of peroxisome proliferator-activated receptor delta in colorectal cancer. *Proc Natl Acad Sci USA* **97**:13275–13280.

Harmon GS, Lam MT, and Glass CK (2011) PPARs and lipid ligands in inflammation and metabolism. *Chem Rev* **111**:6321–6340.

Hodgkinson CP and Ye S (2003) Microarray analysis of peroxisome proliferator-activated receptor-γ induced changes in gene expression in macrophages. *Biochem Biophys Res Commun* **308**:505–510.

Hong F, Xu P, and Zhai Y (2018) The opportunities and challenges of peroxisome proliferator-activated receptors ligands in clinical drug discovery and development. *Int J Mol Sci* **19** DOI: 10.3390/ijms19082189.

Hughes TS, Giri PK, de Vera IM, Marciano DP, Kuruvilla DS, Shin Y, Blayo AL, Kamenecka TM, Burris TP, Griffin PR, et al. (2014) An alternate binding site for PPARγ ligands. *Nat Commun* **5**:3571.

Kim HY, Kim HK, Kim JR, and Kim HS (2005) Upregulation of LPS-induced chemokine KC expression by 15-deoxy-delta12,14-prostaglandin J2 in mouse peritoneal macrophages. *Immunol Cell Biol* **83**:286–293.

Kourtidis A, Srinivasaiah R, Carkner RD, Brosnan MJ, and Conklin DS (2009) Peroxisome proliferator-activated receptor-gamma protects ERBB2-positive breast cancer cells from palmitate toxicity. *Breast Cancer Res* **11**:R16.

Larigauderie G, Cuaz-Pérolin C, Younes AB, Furman C, Lasselin C, Copin C, Jaye M, Fruchart J-C, and Rouis M (2006) Adipophilin increases triglyceride storage in human macrophages by stimulation of biosynthesis and inhibition of beta-oxidation. *FEBS J* **273**:3498–3510.

Lea MA, Sura M, and Desbordes C (2004) Inhibition of cell proliferation by potential peroxisome proliferator-activated receptor (PPAR) gamma agonists and antagonists. *Anticancer Res* **24** (5A):2765–2771.

Lee C-H, Kang K, Mehl IR, Nofsinger R, Alaynick WA, Chong L-W, Rosenfeld JM, and Evans RM (2006) Peroxisome proliferator-activated receptor delta promotes very low-density lipoprotein-derived fatty acid catabolism in the macrophage. *Proc Natl Acad Sci USA* **103**:2434–2439.

Lee G, Elwood F, McNally J, Weiszmann J, Lindstrom M, Amaral K, Nakamura M, Miao S, Cao P, Learned RM, et al. (2002) T0070907, a selective ligand for peroxisome proliferator-activated receptor gamma, functions as an antagonist of biochemical and cellular activities. *J Biol Chem* **277**:19649–19657.

Leesnitzer LM, Parks DJ, Bledsoe RK, Cobb JE, Collins JL, Consler TG, Davis RG, Hull-Ryde EA, Lenhard JM, Patel L, et al. (2002) Functional consequences of cysteine modification in the ligand binding sites of peroxisome proliferator activated receptors by GW9662. *Biochemistry* **41**:6640–6650.

Lefebvre P, Chinetti G, Fruchart J-C, and Staels B (2006) Sorting out the roles of PPAR alpha in energy metabolism and vascular homeostasis. *J Clin Invest* **116**: 571–580.

Li AC, Binder CJ, Gutierrez A, Brown KK, Plotkin CR, Pattison JW, Valledor AF, Davis RA, Willson TM, Witztum JL, et al. (2004) Differential inhibition of

macrophage foam-cell formation and atherosclerosis in mice by PPARalpha, beta/delta, and gamma. *J Clin Invest* **114**:1564–1576.
Luquet S, Gaudel C, Holst D, Lopez-Soriano J, Jehl-Pietri C, Fredenrich A, and Grimaldi PA (2005) Roles of PPAR delta in lipid absorption and metabolism: a new target for the treatment of type 2 diabetes. *Biochim Biophys Acta* **1740**: 313–317.
Maess MB, Buers I, Robenek H, and Lorkowski S (2011) Improved protocol for efficient nonviral transfection of premature THP-1 macrophages. *Cold Spring Harb Protoc* **2011**:pdb.prot5612.
Maess MB, Sendelbach S, and Lorkowski S (2010) Selection of reliable reference genes during THP-1 monocyte differentiation into macrophages. *BMC Mol Biol* **11**: 90.
Maeß MB, Wittig B, Cignarella A, and Lorkowski S (2014) Reduced PMA enhances the responsiveness of transfected THP-1 macrophages to polarizing stimuli. *J Immunol Methods* **402**:76–81.
Magadum A and Engel FB (2018) PPARβ/δ: linking metabolism to regeneration. *Int J Mol Sci* **19** DOI: 10.3390/ijms19072013.
Moore KJ, Rosen ED, Fitzgerald ML, Randow F, Andersson LP, Altshuler D, Milstone DS, Mortensen RM, Spiegelman BM, and Freeman MW (2001) The role of PPAR-gamma in macrophage differentiation and cholesterol uptake. *Nat Med* **7**:41–47.
Neels JG and Grimaldi PA (2014) Physiological functions of peroxisome proliferator-activated receptor β. *Physiol Rev* **94**:795–858.
Nicholson AC and Hajjar DP (2004) CD36, oxidized LDL and PPAR gamma: pathological interactions in macrophages and atherosclerosis. *Vascul Pharmacol* **41**: 139–146.
Nielsen R, Grøntved L, Stunnenberg HG, and Mandrup S (2006) Peroxisome proliferator-activated receptor subtype- and cell-type-specific activation of genomic target genes upon adenoviral transgene delivery. *Mol Cell Biol* **26**: 5698–5714.
Paul A, Chang BH-J, Li L, Yechoor VK, and Chan L (2008) Deficiency of adipose differentiation-related protein impairs foam cell formation and protects against atherosclerosis. *Circ Res* **102**:1492–1501.
Reilly SM and Lee C-H (2008) PPAR delta as a therapeutic target in metabolic disease. *FEBS Lett* **582**:26–31.
Robenek H, Robenek MJ, Buers I, Lorkowski S, Hofnagel O, Troyer D, and Severs NJ (2005) Lipid droplets gain PAT family proteins by interaction with specialized plasma membrane domains. *J Biol Chem* **280**:26330–26338.
Schnoor M, Buers I, Sietmann A, Brodde MF, Hofnagel O, Robenek H, and Lorkowski S (2009) Efficient non-viral transfection of THP-1 cells. *J Immunol Methods* **344**: 109–115.
Seimandi M, Lemaire G, Pillon A, Perrin A, Carlavan I, Voegel JJ, Vignon F, Nicolas J-C, and Balaguer P (2005) Differential responses of PPARalpha, PPARdelta, and PPARgamma reporter cell lines to selective PPAR synthetic ligands. *Anal Biochem* **344**:8–15.
Shearer BG, Wiethe RW, Ashe A, Billin AN, Way JM, Stanley TB, Wagner CD, Xu RX, Leesnitzer LM, Merrihew RV, et al. (2010) Identification and characterization of 4-chloro-N-(2-[5-trifluoromethyl)-2-pyridyl]sulfonylethyl)benzamide (GSK3787), a selective and irreversible peroxisome proliferator-activated receptor delta (PPARdelta) antagonist. *J Med Chem* **53**:1857–1861.
Stolle K, Schnoor M, Fuellen G, Spitzer M, Cullen P, and Lorkowski S (2007) Cloning, genomic organization, and tissue-specific expression of the RASL11B gene. *Biochim Biophys Acta* **1769**:514–524.
Stolle K, Schnoor M, Fuellen G, Spitzer M, Engel T, Spener F, Cullen P, and Lorkowski S (2005) Cloning, cellular localization, genomic organization, and tissue-specific expression of the TGFbeta1-inducible SMAP-5 gene. *Gene* **351**:119–130.
Tong L and Harwood HJ Jr (2006) Acetyl-coenzyme A carboxylases: versatile targets for drug discovery. *J Cell Biochem* **99**:1476–1488.
Tontonoz P, Nagy L, Alvarez JG, Thomazy VA, and Evans RM (1998) PPARgamma promotes monocyte/macrophage differentiation and uptake of oxidized LDL. *Cell* **93**:241–252.
Tontonoz P and Spiegelman BM (2008) Fat and beyond: the diverse biology of PPARgamma. *Annu Rev Biochem* **77**:289–312.
Varga T, Czimmerer Z, and Nagy L (2011) PPARs are a unique set of fatty acid regulated transcription factors controlling both lipid metabolism and inflammation. *Biochim Biophys Acta* **1812**:1007–1022.
Vosper H, Patel L, Graham TL, Khoudoli GA, Hill A, Macphee CH, Pinto I, Smith SA, Suckling KE, Wolf CR, et al. (2001) The peroxisome proliferator-activated receptor delta promotes lipid accumulation in human macrophages. *J Biol Chem* **276**: 44258–44265.
Vrablík M and Češka R (2015) Treatment of hypertriglyceridemia: a review of current options. *Physiol Res* **64** (Suppl 3):S331–S340.
Wallert M, Schmölz L, Koeberle A, Krauth V, Glei M, Galli F, Werz O, Birringer M, and Lorkowski S (2015) α-Tocopherol long-chain metabolite α-13′-COOH affects the inflammatory response of lipopolysaccharide-activated murine RAW264.7 macrophages. *Mol Nutr Food Res* **59**:1524–1534.
Wang Y-X (2010) PPARs: diverse regulators in energy metabolism and metabolic diseases. *Cell Res* **20**:124–137.
Zhang X, Goncalves R, and Mosser DM (2008) The isolation and characterization of murine macrophages, *Curr Protoc Immunol* **Chapter 14**, p Unit 14.1.

Address correspondence to: Dr. Stefan Lorkowski, Institute of Nutrition, Friedrich Schiller University Jena, Dornburger Str. 25, 07743 Jena, Germany. E-mail: stefan.lorkowski@uni-jena.de